The Analysis of Reinforced Soil under Strip Foundation by Measurement of the Displacement Vectors by the Means of Image Processing

Forough Ashkan✎⊠

Department of Civil Engineering, Faculty Member of Engineering, University of Maragheh, Iran

✎Corresponding author's Email: ashkan@maragheh.ac.ir

ABSTRACT

Reinforcing soil for solving the geotechnical problems is a very useful and economical technique. Soil as a grainy environment has a very good resistance under pressure and when it is cut, but is not that much resistant when being pulled. Being reinforced due to increase of the friction, it will be more resistant when being cut. I this survey we leveled our focus on the analysis of modeling loose sand and using image process for measuring the displacement Vectors and also, investigating the effect of different factors such as reinforced type and layer on the soil failure mechanics and we compared consequences with unreinforced status of the soil. The results convey this very message that the surfaces of the soil which were failed and also the depth of mentioned surfaces in reinforced model compared to unreinforced one increase and cover more loading capacity.

Keywords: Reinforced soil, displacement vectors, soil mechanics, image processing.

INTRODUCTION

One of the very important elements when designing foundation of structures such as such as buildings, followed by bridge and dam, is properly evaluated the role of stress-deformation behavior of soil under the Foundation (Bowles 2003). This factor is dependent on soil's mechanical features. The first person deciding to purpose a theory about the calculation of the ultimate bearing capacity of shallow foundation was Terzaghi in 1943. He assumed the shear failure surface under the final strip load like what u see in picture 1.

γ = Special weight; C= Cohesion; Ø= Friction angel
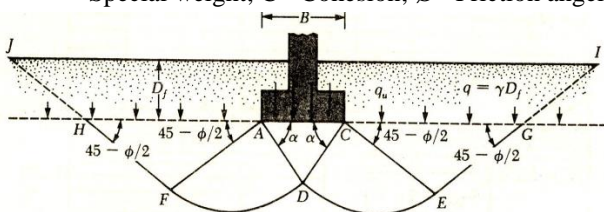

**Figure 1.** The ultimate in bearing shear fissures a rigid rough contact surface with tape infrastructure

He also substituted the existing soil above the surface which was under the foundation with overload in degree of $q = \gamma D_f$ (in which γ is the special weight of the soil.).

The failure area under the foundation can be divided into areas as goes below:

1. Triangular area immediately below the Foundation (wedge disruptive).

2. Radial shear regions of the ADF and the CDE with curved fissures DF and DE.

3. Two Rankin-triangular area AFH and CEG.

Terzaghi (1943) deemed that angels of CAD and ACD is equal to inner friction angel to Ø.

Huang and Meng (1997) suggested a theory about the reinforced soil failure mechanics according to cutting mechanics of wide-slab in soil which was recommended by and or Schlosser et al. (1983) which is illustrated through picture 2 (El Sawwaf and Nazir, 2012; Lackner et al. 2013; Chen and Abu-Farsakh, 2015). Fallowing after this very theory failure separation force after reinforced layer is (B+Δ B) and failure areas of resistance increase even to soil surface.
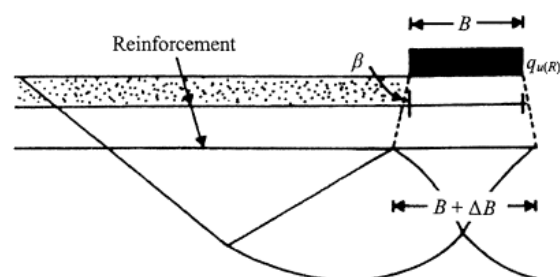
Picture 2. Slab-wide mechanism in reinforced soil under the strip base

Techniques proffered up until now are based on analytic research and modeling experiments. Almost of the physical models are in line with force - displacement information of the foundation and usually it is a real burden and a very tough challenge to observe failure mechanism. Because of the complex nature of the soil behavior which in turn leads to the complication of the arms and soil action? The analysis of the changed behavior of the appearance of the soil beneath trip bases in the experimental ways will enables us to perceive soil's changed appearance or failure well. This research will equip us with better understanding of different parameters and their effects on slip surface when loading, likewise.

MATERIAL AND METHODS

Features of physical model:

In this research dried sand was utilized for experiment. For determining sand's features, grain size experiments were in compliance with ASTM, D 422-87 special weight according (ASTM D 854-87). The intended sand included 0.02% was sieved with 200 was categorized as bad sand (Asadpour Estiar, 2006).). Other soil parameters are included in table 1. About the precipitation method of the sand for creating homogenous models for loose sand by rain method, sand was poured from the height about 25 cm. In Table1, Features of used sand is observable.

Table 1. Specifications of used sand

ϕ	G_s	$\gamma\left(gr/cm^3\right)$	C_u	C_c
27	2.67	1.5	1.25	0.992
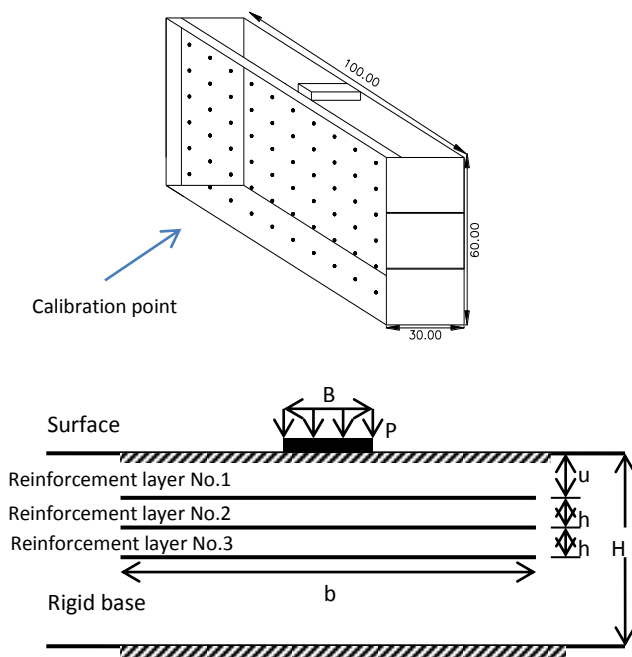
Picture 3A.Parameters of model and experiment box

B)
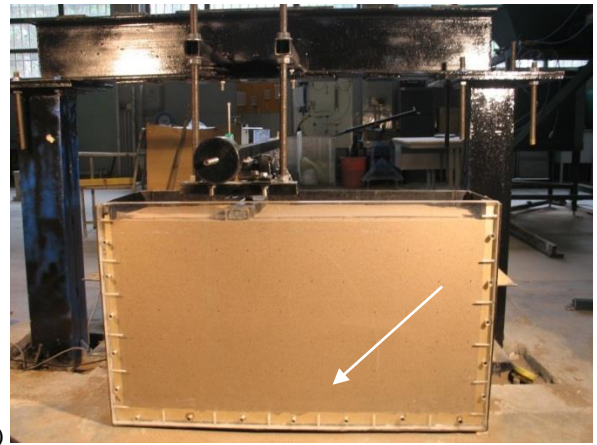
Picture 3B. the base holder of Jak, and the experimental like box.

Picture 3 A Exhibits parameters of the model, experiment box and the way by which the foundation of the soil was enhanced for implementing the load. A rigid frame was designed and used in laboratory.

First, a trip basis with 1.8 m length 0.40 width and 0.50 height was made and in two extremes of this base, the plate was installing the bases accompanying with 6bolt.

In this vein the installation and attaching points were designed. As picture conveys the message, for bases we employed attachment of the two pipe UNP160 and for the beam attachment of the two pipe UNP200 are utilized and later on the beam and the columns were fortified by the belt and bracket.

Pic 3. B. reveals force system of the base holder.

For building experimental plate which was supposed to contain the soil. We used iron pages with thickness of 3.9mm with the size of (1*0.3*0.6m).

For photographing the system while loading continuously, outside of the box was planned out of talc with thickness of 3cm.

For the purpose of the force controlling there is a system by adding Kent ledges tries to monitor the force and adds to the force till the failure point of the system.

Due to the reduction of the loading operation, a system like a lever was taken advantage of which has an arm in size about 1.1*0.03 m and thickness of 0.03m and a load of 3 kg in order to balance the system was added.

The schematic picture of loading system and types of supports has been presented in Figure 4. The space between weights to loading place is 0.75cm and in each loading the load will be 9.3 times added to the previous load of the system.
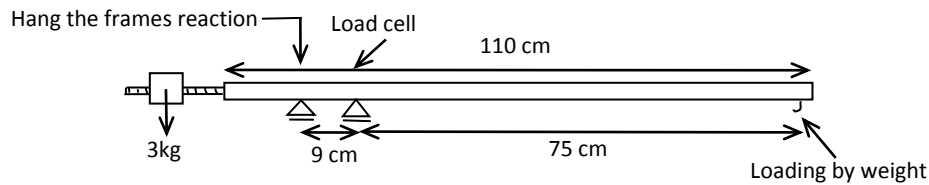
Figure 4. The schematic picture of loading system and types of supports

For passing the force of the load to the soil experimented, a rigid frame in 0.3m*0.061m dimensions was deployed as a surface of trip base on the soil bed. For estimating the load, digital local cell of 250 kg capacity was in place. In experimental model, the load cell was located precisely at center of the iron plate and compromised the whole consistent system. In order of calculating of the settlement of the bases a displacement sensor or LVDT was used which was a plate right in the center. Present research comprises 4 experiments of loading. In order to reinforcing soil foundation exploitation of a particular reinforced called Geotextile was work.

The altering parameters goes as; number of reinforced layers (N), the depth of the reinforced layer (U), The width of the reinforced layers (B), The distance between the reinforced layers (H). In table 2 You may explore features of the experimental models.

Table 2. the features of testing models

Test number	1	2	3	4
Reinforcement	Geotextile	-	Geotextile	Unreinforced
N	1	-	1	2
b/B	9	-	9	9
u/B	0.5	-	0.5	0.5
h/B	-	-	-	0.5
Calibration factor	0.232	0.217	0.256	0.257

Image processing:

While carrying out the experiment by PIV pictorial method which was first exploited by Adrian1991 in the experimental studies in fluid mechanics and recently has been employed in studying and examining changes of the appearance of the soil which is changing by White et al. (2003, 2004).

Pictures are taken by the means of the digital camera with 7.1 mega pixel clarity $(3072*2304)$ and are saved to be processed afterwards by Geopiv8 software.

In order to process the pictures by PIV method, all pictures should be divided into Mesh and each of these Meshes has special picture structure and this will aid in other pictures to find the exact location of other Mesh. The displacement of every Mesh is clear and compared to first is calculable. These are in pixel so one may need to turn them into millimeter so the Calibration points are needed.

These places are exhibited on observation widow with black color in particular distances in millimeter.

Calibration points are findable by means of the Close- range photogrammetry and as a result of clear distances from each other and the stable location of the Calibration points during the experiment, it was possible to apply locations of the Meshes. The displacement vectors reached by near board photogrammetry and are transferable from the picture site to the real one. So the displacement field of the soil plate is achieved.

In this study, analyses were drawn by Meshing of the taken photos $(48*48)$ and nice picture structures were gained and accordingly the shift of the sites of the Meshes in soil mass was evaluated.

RESULTS AND DISCUSSION

In picture5 displacement vectors of the settlement of the trip base located on loose sand in loading plate is obvious.

The levels of the settlement are S/B=0.2, 0.35, 0.5.

The settlement diagram are horizontal and pressure on one layer has been chosen as Geogrid.

In this diagram, the status of the loading plate are shown according to settlement. The dark line exhibits the Geogrid layer before the deformation (Saket, 2006).

The shift of the soil elements for every status from the beginning till the intended settlement are displayed.

It is clear that in all the cases displacement vectors beneath the foundation is inclined to downward and toward the sides. Since the soil is loose the willingness for condensation under the base is observable and the displacement vectors under the base are bigger than the rest causing the reinforce under the base to change appearance and the other discernable issue is the movement of the elements of the soil when increasing amount of the loading is heightened.

When displacement vectors extended failure wedge and shear zone are formed beneath the base and in these areas the vectors inclined upwards. Above the reinforced layer, the angel of the displacement vectors is not in line with the vectors under the reinforced layer and also above the reinforced layer local failure areas are shaped.
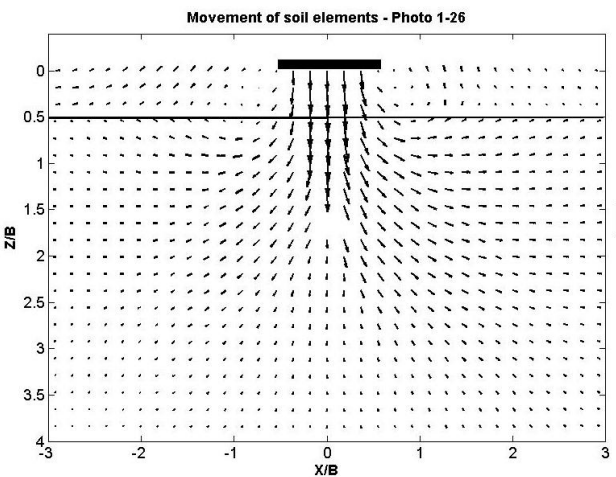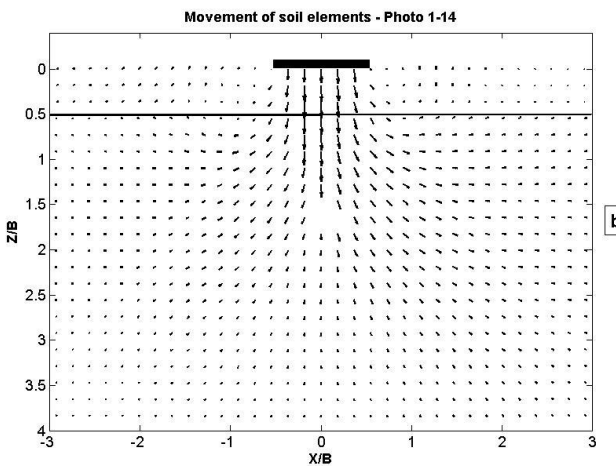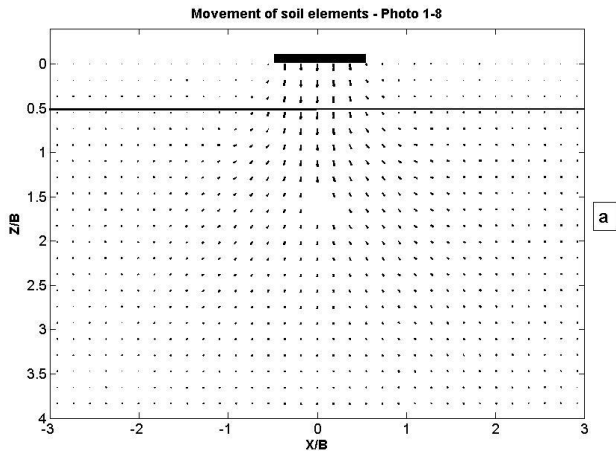
Picture 5. Displacement vectors in soil (a S/B=0.2 ، (b S/B=0.35 ، (c S/B=0.5 .Test 1

In picture 6, The shear strain induced with the loading plate's settlement in settlement levels in **S**/B=0.2, 0.35, 0.5. Has been showed. The maximum of which is going to be achieved through below equation:

$$\gamma_{max} = \sqrt{(\varepsilon_x - \varepsilon_y)^2 + \gamma_{xy}^2},$$

(1)

In which:

$$\varepsilon_x = \frac{\partial u}{\partial x} + \frac{1}{2}\left[\left(\frac{\partial u}{\partial x}\right)^2 + \left(\frac{\partial v}{\partial x}\right)^2\right],$$

(1)

$$\varepsilon_y = \frac{\partial v}{\partial y} + \frac{1}{2}\left[\left(\frac{\partial u}{\partial y}\right)^2 + \left(\frac{\partial v}{\partial y}\right)^2\right],$$

(1)

$$\gamma_{xy} = \frac{\partial u}{\partial y} + \frac{\partial v}{\partial x} + \left(\frac{\partial u}{\partial x}\frac{\partial u}{\partial y} + \frac{\partial v}{\partial x}\frac{\partial v}{\partial y}\right).$$

(1)

In this picture one can behold that The amassed strain which has been made is expanded by the increase of the settlement of the loading plate in width and length direction and in 30 mm settlement there is strain up until the depth of Z/B=2 and in width -0.5<X/B<0.5. In the Geogrid also there is shear strain.

While in S/B=0.2 amass of the maximum shear strain is distinct in sides of the base. It is due to the looseness of the soil and there is an inclination of condensation in the soil and so base settles in the soil and cutting failure of the Punch takes place and amass of the maximum cutting strain explanatory of the existence of slip surface in that very location.
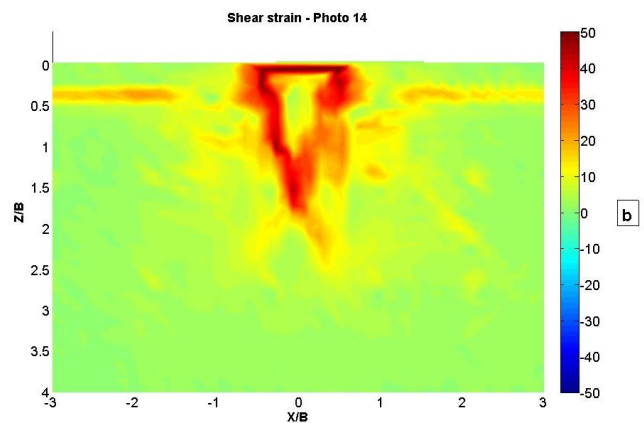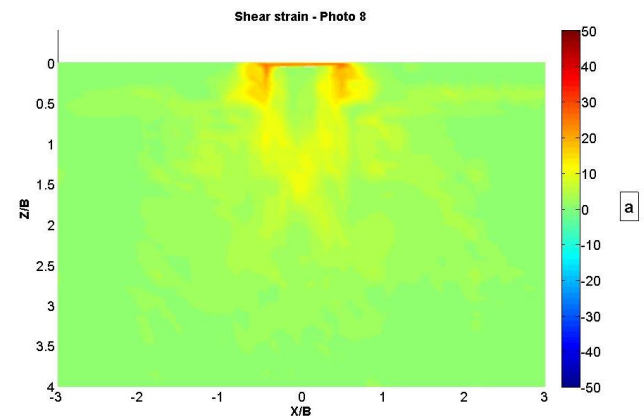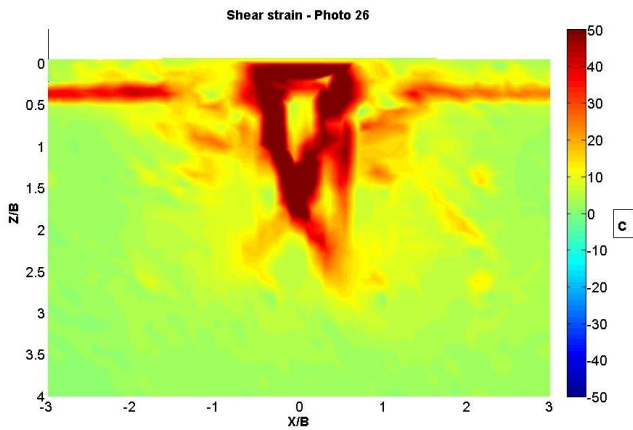
Picture 6. S/B=0.2 ، (b S/B=0.35 ، (c S/B=0.5) .Test 1 . maximum shear strain

Gradually by expanding the depth shift vectors is downward and their sizes reduced. For the analysis of the failure wedge and shear zone and resistant formed in soil, one and two reinforced layer and foundation of the displacement vectors , the experiments numbers12,19,20 are compared and completely schematical images of how these reinforces have effect on the failure mechanics of the soil have been depicted. Picture 7, shows displacement vectors in an unreinforced foundation.
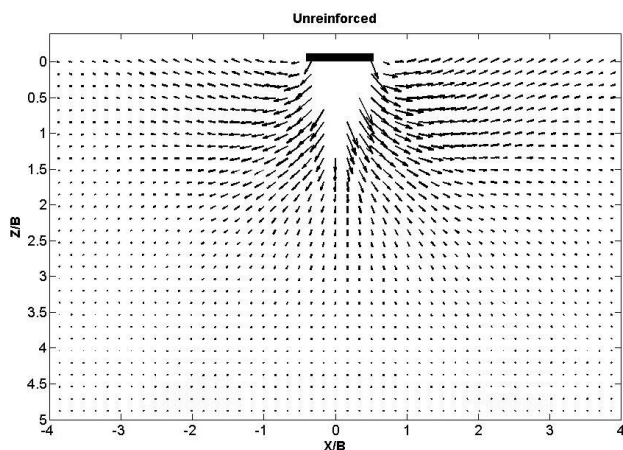
Picture 7. Failure surfaces of unreinforced soil.

Due to the looseness of the soil, no complete Terzaghi failure mechanics of the soil is seen, but a mechanics in between of failure and settlement simultaneously occur.

By adding to the depth, Vectors toward down is observable and their sizes is reduced.

Area of $_{-0.9} \langle x/_B \langle _{0.9}$ in Z/B=0.5, is in Active

triangle Rankin area and shear zone.

In these areas the direction of the displacement vectors is first toward down and then upward.

In picture 8, you can see the displacement vectors in enhances foundation with one layer of reinforce.

The dark line shows Geotextile reinforced before deformation. It is so discernable that the direction of the displacement vectors in the reinforced layer is downward. In this section, the size of the vectors is bigger and resulting in deformation the reinforced layer under the foundation. In half right of the soil model in depth of Z/B=1, and 3.72<X/B<2.11 is gradually shifting upward. Failure wedge increasingly after the reinforced layer of the Geotextile started to form. Above the reinforced layers, the angle of the displacement vectors is not in line with reinforced layers' vectors.

Also above the Geotextile layer surface of the local failure has been shaped which are conspicuous with red color in the picture. The slip layers caused in reinforced foundation does not corresponds with the suggested slip layers. According to the wide-slab failure mechanism in Z/B=0.5 depth, the size of the triangle area under the reinforced layer is (ΔB) ،and also is $B + \Delta B$ bigger than the width and likewise the area of $_{-2.11} \langle x/_B \langle _{2.11}$ in

Z/B=1 is in the shear zone and active triangle Rankin area.

In these areas the direction of the displacement vectors is toward down and horizontal, also in an enhanced cases, the failure surfaces reached to the reinforced under layers and are not transferred to the surface of the earth. Agreeing with the diagram the incorrectness of the Huang and Meng theory has been confirmed.
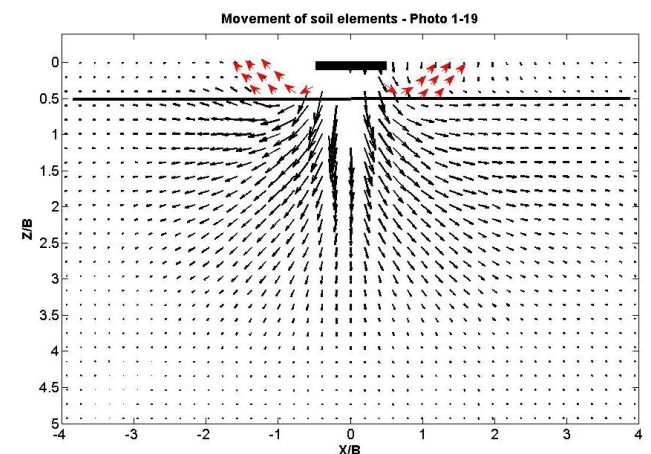
Picture 8. Failure surfaces in an enhanced sol with a layer of (S/B=0.5). Test3

Picture 9 happens to show displacement vectors in an enhanced foundation with two reinforced layers. Dark lines are showing two layers before the deformation. The thing which transparent is that the direction of the displacement vectors under the reinforced layer is upward.

The displacement vectors in shear zone and the resistant areas gradually shift to up. The failure wedge is beginning to be formed under the second reinforced layer. In between of two reinforced layers the failure surfaces which are depicted by red color vectors.

The slip surface in the reinforced soil foundation with 2 layers does not comply with the slip surface of Terzaghi. According to the failure wide- slab in Z/B=1 depth, the size of the triangle areas under the reinforced layer is ΔB and ($B+\Delta B$) times increases compared to the base, furthermore the area of $-1.91 \langle \frac{x}{B} \langle 1.91$ in Z/B=1.52 is part of active triangle Rankin area and shear zone.

In the mentioned areas the direction of the displacement vectors is to down and also is horizontal. Besides, in enhanced cases with the short reinforced width. The failure areas reached up to the reinforced layer. This survey makes it known that when loading increased the tip of the failure wedge turned to the left and the soil beneath the base merely is scattered from one side.

This experiment was repeated several times and probable conclusion are below:

The force system was not balanced. This system was installed to the rigid frame by two buckles. It is possible to check its balance with the eyes but errors may occur while balancing it with the eyes. The force on the base was out of the center. The force of the base is on the Load cell which is in center of the iron plate. Due to the implementing it by hands, there may be some imprecision. So, the load may be was not exactly at center.

Inconsistency of the soil beneath the base which is of least important compared to the two previously mentioned cases above.
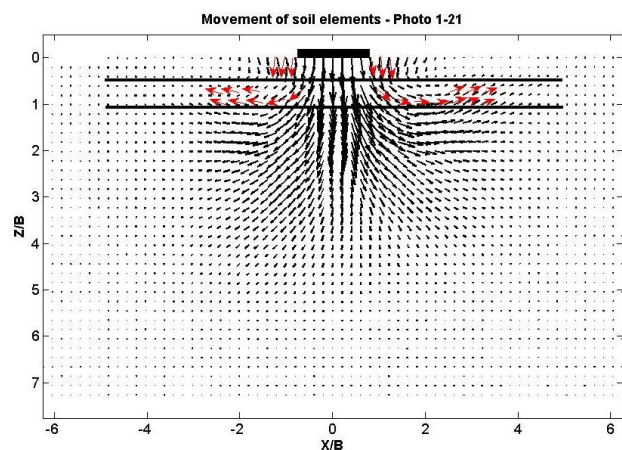
Picture 9. Test 4. Failure surfaces in soil reinforced with two layers.(S/B=0.5)

By comparing the two pictures of 7- 9 we can conclude that increase of the reinforced layers results in failure of the surface and makes it (failure surface) to be wider and deeper when we reinforced the soil with two layers meaning that failure surface in enhanced cases with two reinforced layers is longer and huge mass of reinforced soli are in action and more loading capacity is being covered in this very case.

DECLARATIONS

Authors' Contributions
All authors contributed equally to this work.

Competing interests
The authors declare that they have no competing interests.

REFERENCES

Asadpour Estiar R (2006). Experimental study of the effect of reinforcement on the mechanical behavior of sand. MSc Thesis, Faculty of Engineering, University of Tabriz.

Bowles, Joseph E. (2003). Foundation analysis and design, McGraw-Hill Inc.

Chen Q and Abu-Farsakh M (2015). Ultimate bearing capacity analysis of strip footings on reinforced soil foundations. Original Research Article Soil and Foundations, Volume 55, Pages 74-85.

El Sawwaf M and Nazir AK (2012). The effect of deep excavation-induced lateral soil movements on the behavior of strip footing supported on reinforced sand. Original Research Article. Journal of Advanced Research, Volume 3, Issue 4, Pages 337-344.

Huang CC and Menq FY (1997). Deep footing and wide-slab effects on reinforced sandy ground. Journal of Geotechnical and Geoenvironmental Engineering, ASCE 123 (1), 30–36.

Lackner C and Bergado DT and Semprich S (2013). "Prestressed reinforced soil by geosynthetic-concept and experimental investigations". Original Research Article Geotextiles and Geomembranes, Volume 37, Pages 109-123.

Saket A (2006). Geogrid and its application", the Ministry of Industry and Mines, Geological and Mineral Exploration.

Schlosser F, Jacobsen HM and Juran I. (1983). Soil reinforcement. General Report, VIII European Terzaghi K (1943). Theoretical Soil Mechanics. Wiley, Inc., New York.

White DJ and Take WA and Bolton MD (2003). Soil deformation measurement using particle image velocimetry (PIV) and photogrammetry. Géotechnique 53, No. 7, 619-631.

White DJ and Richards and Lock AC (2004). The measurement of landfill settlement using digital imaging and PIV analysis. Schofield Center, Department of Engineering, University of Cambridge, UK.

Conference on Soil Mechanics and Foundation Engineering, Balkema, Helsinki, 83-101.